Liquid-State Processes

- **In Situ composites**

1-By eutectic reactions

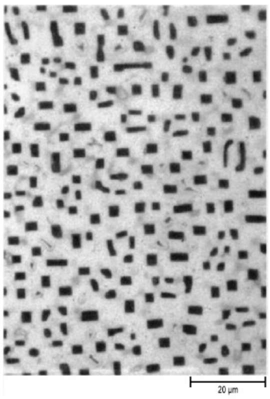

Fig. 5.11 Example of a fibrous eutectic microstructure with a small volume fraction of one phase (molybdenum fibers in NiAl matrix). Transverse section of a directionally-solidified (DS) sample. As-polished. Courtesy of E. Blank. Source: Ref 5.6

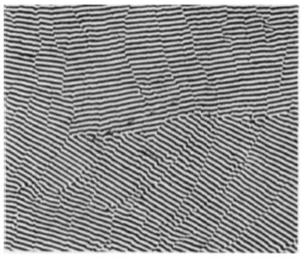

Fig. 5.10 Example of a lamellar eutectic microstructure (Al-Al_2Cu) with approximately equal volume fractions of the phases. Transverse section of a directionally-solidified (DS) sample. As-polished. Source: Ref 5.6

Table 6.2 Some important in situ composite systems

System	Carbide (vol. %)	T_E[a] (°C)
Co–NbC	12	1,365
Co–TiC	16	1,360
Co–TaC	10	1,402
Ni–HfC	15–28	1,260
Ni–NbC	11	1,330
Ni–TiC	7.5	1,307

[a] T_E is the eutectic temperature

- **In Situ composites**

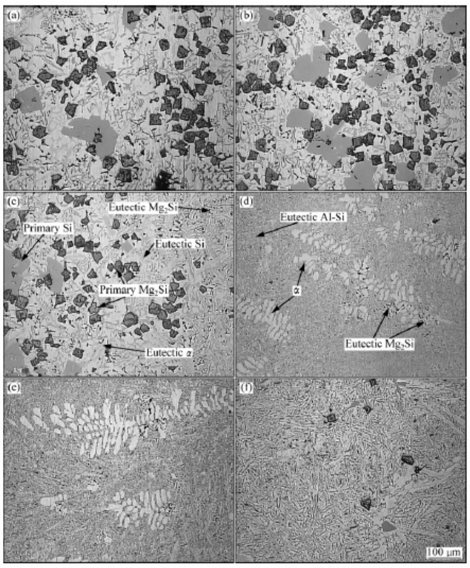

Fig.6 SEM images of Al-19Si-5Mg tube in Fig.2(b): (a) 1−3 mm; (b) 3−5 mm; (c) 5−8 mm; (d) 8−10 mm; (e) 10−14 mm; (f) 14−15 mm)

Liquid-State Processes

- **In Situ composites**

- Reinforcements are formed during the solidification of the molten metal, e.g., controlled unidirectional solidification of eutectic alloys.

- Fineness and distribution of the reinforcement phase is controlled by the solidification rate.

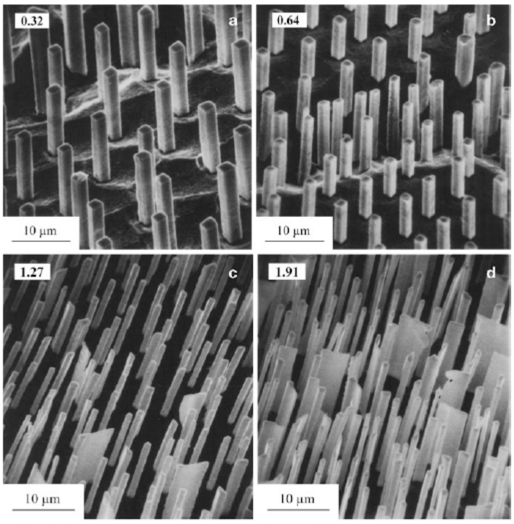

Fig. 6.9 Transverse sections of in situ composites obtained from a eutectic at different solidification rates indicated in *left-hand top* corners (cm/h). The nickel alloy matrix has been etched away to reveal the TaC fibers. [From Walter (1982), used with permission]

Liquid-State Processes

- **In Situ composites**

2-By chemical reactions

•Aluminothermic type reactions:

Reaction between some elements in the molten matrix and ex-situ added compounds.

Example:

$$\mathbf{ZnO + Al \rightarrow Zn + Al_2O_3}$$

In-situ Al-Al_2O_3 Composite

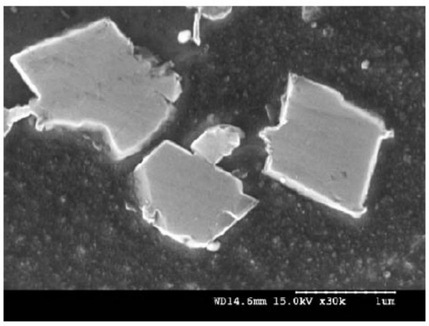

Fig. 9—Nearly defect-free interfaces of alumina particles incorporated in aluminum matrix.

A. Maleki, et al., Met & Mat Trans, 39A, 3034-303, 2008.

Liquid-State Processes

- **In Situ composites**

• **SHS process (self-propagating high-temperature synthesis):**

An exothermic reaction between two components to produce a third component. A master alloy with high Vol% of reinforcement is produced which can be mixed and remelted with a base alloy to produce a desirable amount of particle reinforcement, for example SiC or TiB_2 in an aluminum, nickel, or intermetallic matrix.

Solid-State Processes

Diffusion bonding

- Used to join similar or dissimilar metals
- Stacking in a predetermined order of:
  - ✓Matrix alloy foil and fiber arrays
  - ✓Composite wire
  - ✓Monolayer laminates
- Simultaneous application of pressure and high temperature

  → Inter-diffusion of atoms from clean metal surfaces in contact at elevated temperature

Solid-State Processes

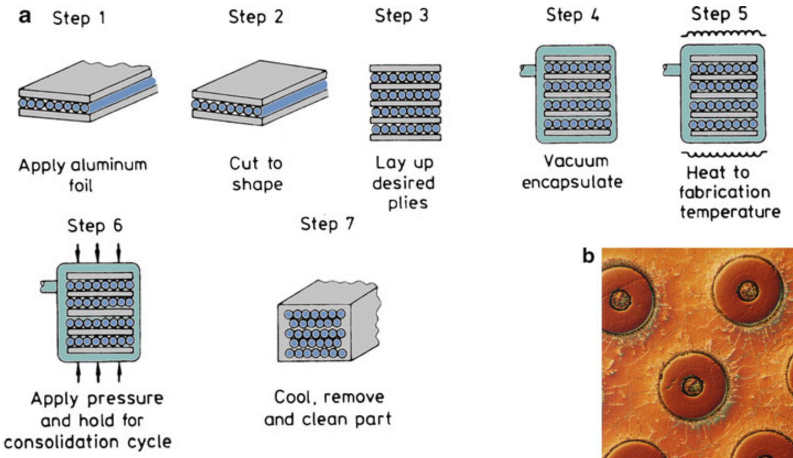

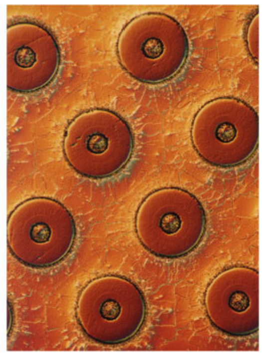

900°C, 105 MPa, 3 h

Fig. 6.8 (a) Schematic of diffusion bonding process.

(b) Microstructure of SiC fiber/titanium matrix composite made by diffusion.
(900 °C, 105 MPa, 3 h, fiber diameter =142 µm)

Solid-State Processes

✓ The main advantages:

- The ability to process a wide variety of matrix metals
- Control of fiber orientation and volume fraction

× The main disadvantages:

- Processing times of several hours
- High processing temperatures and pressures
- Quite expensive
- Only objects of limited size can be produced

Solid-State Processes

Deformation processing of metal/metal composites

✓**Less conventional: In-situ composite**

- Extrusion, drawing, rolling or … of a ductile two-phase material.
- The two phases co-deform → the minor phase elongates and becomes fibrous within the matrix
- The starting material is usually a billet prepared by casting or powder metallurgy methods.

✓**More conventional:**

- **Roll bonding** to produce sheet laminated MMCs
- **ARB** (accumulative roll bonding)
- **CAR** (continual annealing and roll-bonding)

ARB

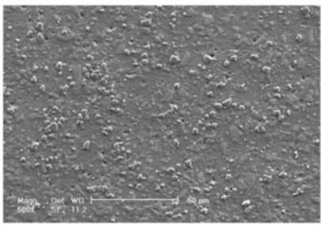

CAR

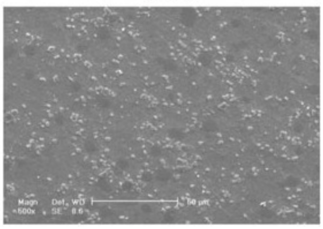

A356/10 vol.% SiC composites
(10 cycles at room temperature)

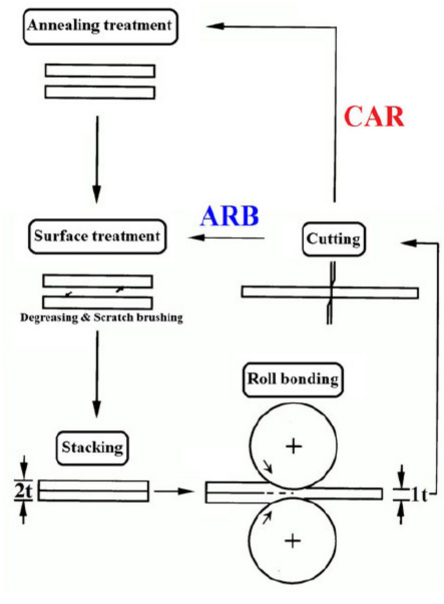

Fig. 2 Schematic illustration of ARB and CAR processes

 R. Jamaati et al., J Mat Eng and Perform 21(7), 2012, 1249-1253.

Solid-State Processes

• ***Nb–Ti composite superconductors***

✓Extremely fine Nb–Ti superconducting filaments embedded in a copper matrix

✓Annealed Nb–Ti rods are inserted into hexagonal-shaped high purity copper tubes.

✓These rods are loaded into a copper tube, evacuated, sealed, and extruded.

✓The extruded rod is cold drawn and annealed repeatedly to the appropriate final size and properties.

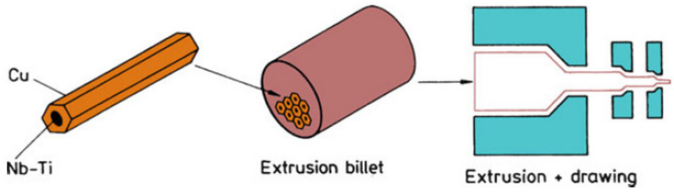

Fig. 9.5 Fabrication route for Nb–Ti/Cu composite superconductors

Solid-State Processes

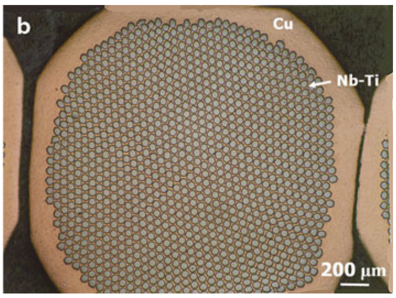

Fig. 9.6 (b) One strand containing 1,060 filaments (Dia. = 50 μm)

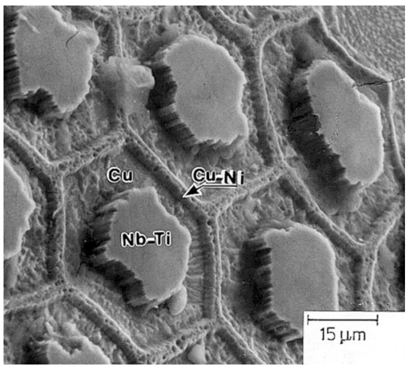

Fig. 9.7 SEM of Nb–Ti/Cu superconductor

Solid-State Processes

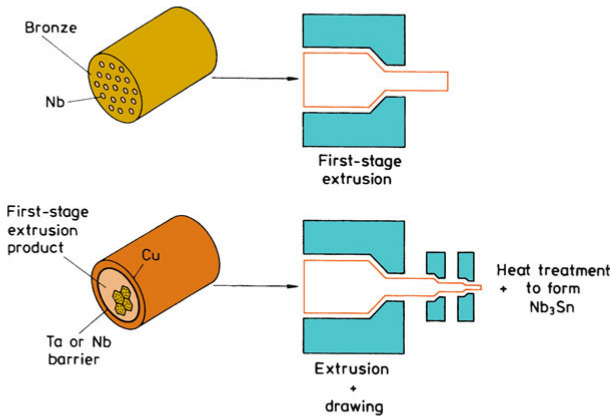

Fig. 9.8 Schematic of the bronze method of fabricating Nb_3Sn/Cu superconductor

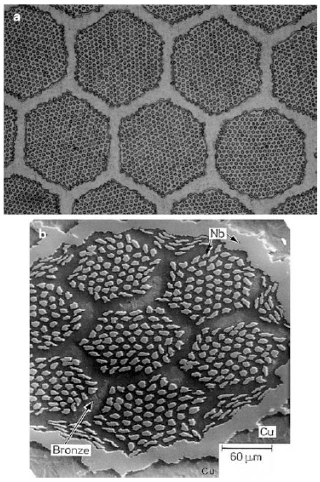

Fig. 9.9 (a) An Nb_3Sn/Cu composite superconductor. Each little dot in the picture is a 4-µm dia. Nb_3Sn filament. (b) SEM of a Nb/bronze composite before the heat treatment to form Nb_3Sn.

Solid-State Processes

Powder metallurgy and extrusion processing

Al/SiC_p composites

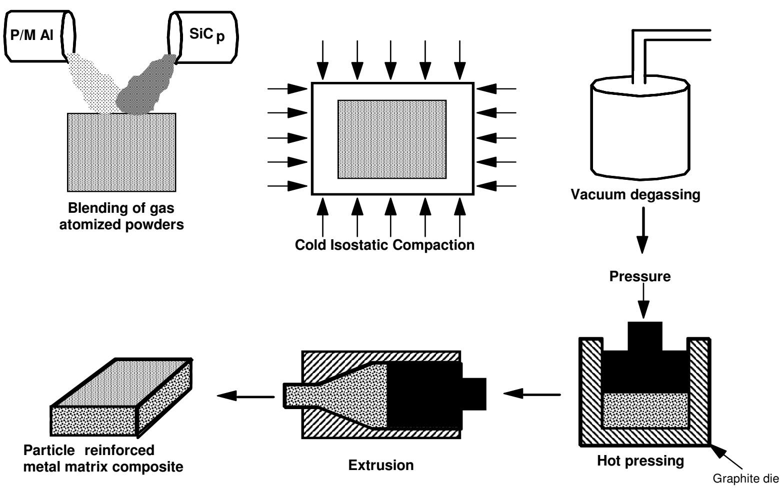

Solid-State Processes

- **Deposition techniques for MMC fabrication**

  1- Coating individual fibers in a tow with the matrix material

  2- Diffusion bonding to form a consolidated composite plate or structural shape

•Several deposition techniques are available:

- ✓Immersion plating (dipping)
- ✓Electroplating
- ✓Spray deposition
- ✓Chemical vapor deposition (CVD)
- ✓Physical vapor deposition (PVD)

(More information available in the text book.)

Main challenges for production of MMCs

1- Porosity (mostly in liquid state processes)

2- Uniform distribution of the reinforcement (agglomeration and segregation issues)

3- Reinforcement/matrix wettability

4- Undesirable reactions between reinforcement/matrix

1- Porosity content of MMCs

Affects mechanical properties, corrosion resistance, surface quality,…

Sources of porosity

- Mechanical entrapment of air during processing, e.g. stirring
- Precipitation of dissolved gases in the melt
- Gas and moisture on the surfaces of the reinforcements
- Moisture on the surfaces of the mould
- Solidification shrinkage

- Higher viscosity of composite slurry→ slower discharge of gas bubbles

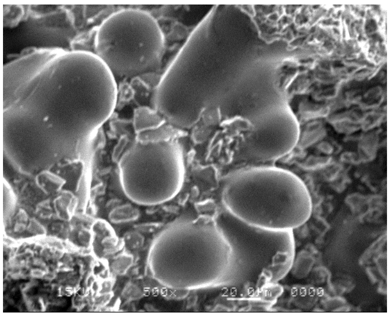

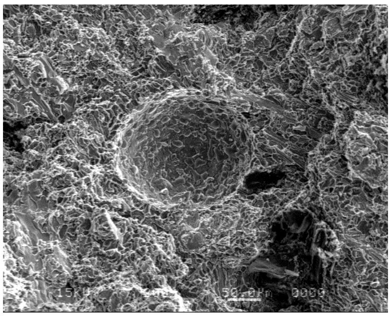

Shrinkage porosity **Gas porosity**
on fracture surfaces of Al-Si alloy/SiC/Graphite composites.

Note: The SiC particles at the interior wall of the gas pore

Gas porosity in cast Al-SiC composite

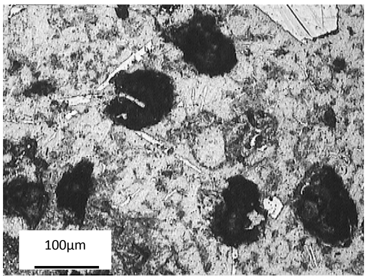

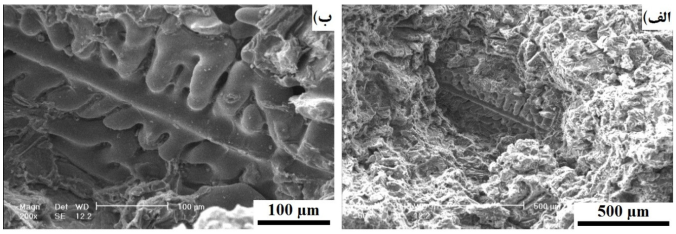

Shrinkage porosity on fracture surface of cast Al-SiC composite

- Process parameters: Stirrer speed, stirrer size, stirrer position in the melt, stirring time, holding time, …
  - For example:
    - Optimum position: 65% of the melt above and 35% below the stirrer
    - Effect of stirring speed on particle incorporation in the matrix:

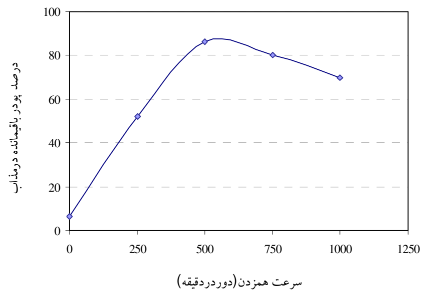

- Porosity increases linearly with the reinforcement content

- Cast MMCs contain large volume of suspended non-metallic particles
  - Large propensity for gas nucleation

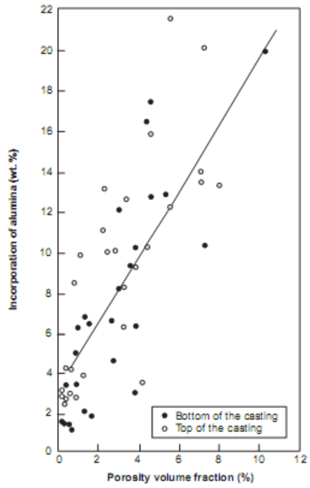

Porosity vol.% versus reinforcement vol.% in cast Al-Al_2O_3

- Reinforcements are covered with a gas layer before coming into contact with the melt
  - The gas layer may persist depending on the wettability of the reinforcement
  - Absorbed moisture on the reinforcements
  - Entrapped gas or moisture between the reinforcement agglomerates
  - Smaller particles→ larger surface area→ higher amount of gas/moisture
  - Moisture can be released by heat treatment at 200-600 °C

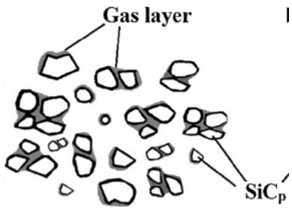

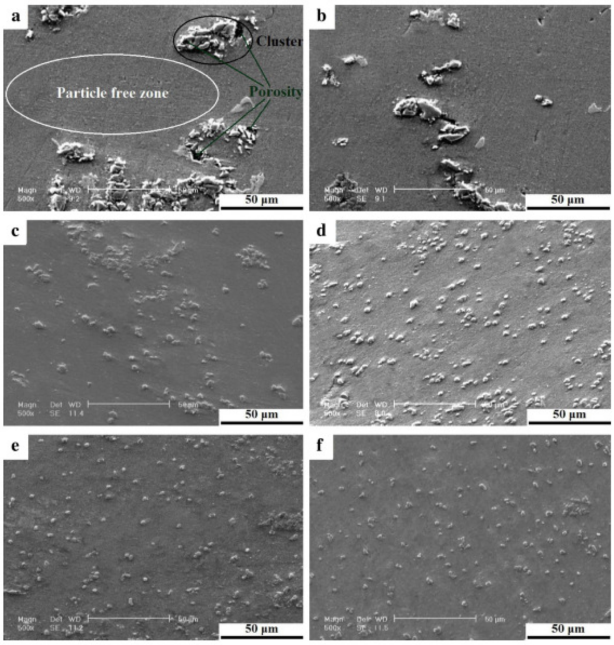

Fig. 2. Typical SEM microstructures of different composites: (a) Al356–SiC_p-650 °C, (b) Al356–SiC_p-607 °C, (c) Al356–(Al–SiC_p)$_{cp}$-650 °C and (d) Al356–(Al–SiC_p)$_{cp}$-607 °C, (e) Al356–(Al–SiC_p–Mg)$_{cp}$-650 °C and (f) Al356–(Al–SiC_p–Mg)$_{cp}$-607 °C.

S. Amirkhanlou, B. Niroumand, Materials Science and Engineering A *528 (2011) 7186– 7195.*

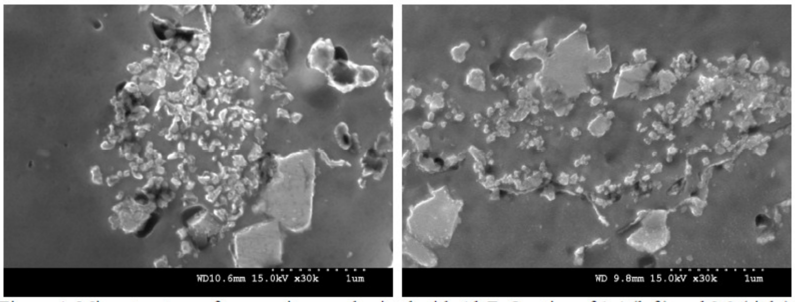

Figure 4: Microstructure of composites synthesized with Al-ZnO ratios of 1:4 (left) and 2:3 (right).

In-situ Al-Al_2O_3

Interface porosity is the most damaging to the mechanical properties

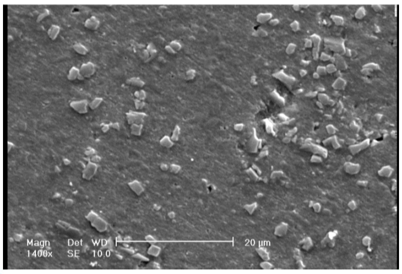

Al-SiC_p

Methods for porosity reduction

- Optimizing the process variables and set-up design
- Increasing reinforcement/melt wettability
- Optimizing reinforcement addition method
- Compocasting
- Vacuum casting
- Squeeze casting
- Post casting deformation processes, e.g. rolling, extrusion, …

2- Uniform distribution of the reinforcement

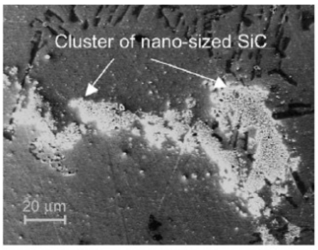

Common defect in *vortex method*:

- Agglomeration due to Van der Waals forces
- Gravity segregation due to density difference
- Reinforcement pushing to the grain boundaries

Particle distribution:

- During stirring: process parameters, wettability, …
- After stirring and before casting: density difference, viscosity, wettability, …
- During solidification: particles redistribution , e.g. engulfment, pushing, …

Particle addition to the melt:

- On the melt surface
- Under the melt surface using a carrier gas
- Spray casting
- Ultrasonic treatment of the slurry
- Dilution of a high vol.% MMC in a melt
- …

Particle addition under the melt surface using a carrier gas

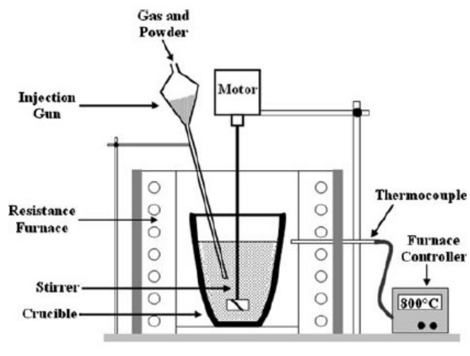

Fig. 1—Experimental setup for slurry preparation.

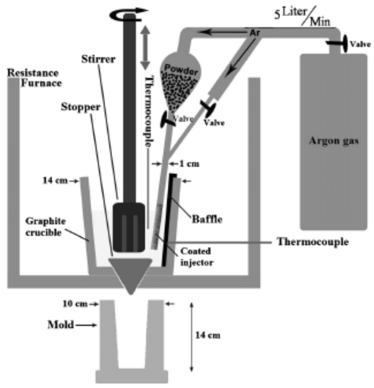

Fig. 1. Schematic of the experimental set-up used in production of the composites.

Ultrasonic dispersion:
- Cavitation
- Acoustic streaming

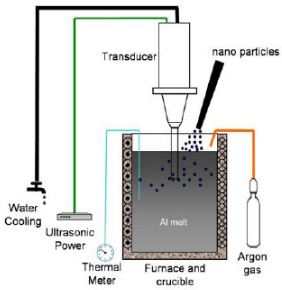

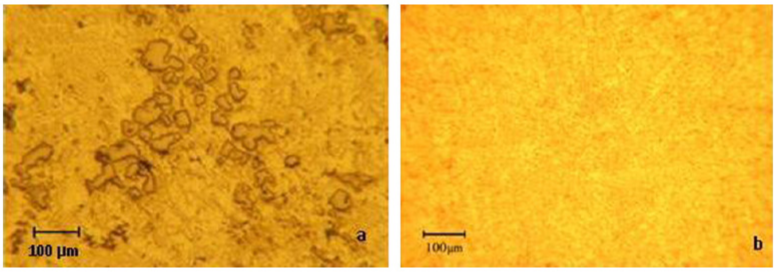

Fig. 15. Microstructure of samples containing 1.5% nanoparticles of SiC_{np}: (a) without ultrasonic treatment and (b) after two 20 min periods of HIDUT.

M.R. Dehnavi, et al., Materials Science & Engineering A, 617(2014)73–83.

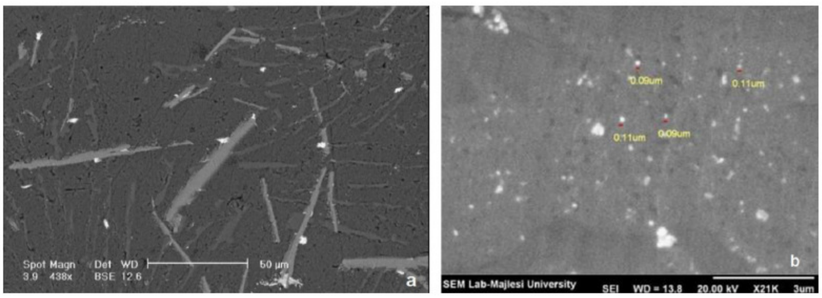

Fig. 16. SEM micrographs of samples containing 1.5% nanoparticles of SiC_{np}: (a) without ultrasonic treatment and (b) after two 20 min periods of HIDUT.

M.R. Dehnavi, et al., Materials Science & Engineering A, 617(2014)73–83.

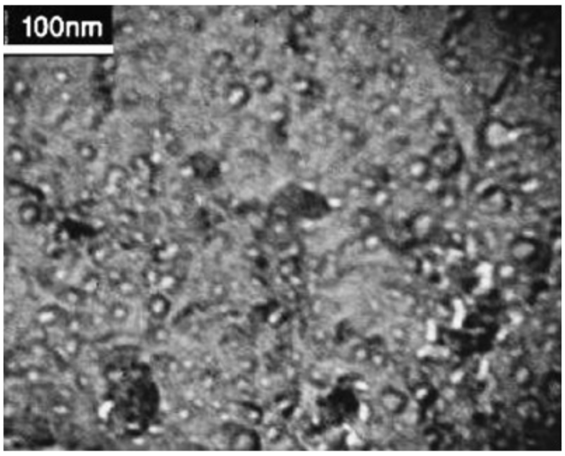

Fig. 17. TEM micrograph of A413–1.5% SiC composite after two 20 min periods of HIDUT.

M.R. Dehnavi, et al., Materials Science & Engineering A, 617(2014)73–83.

Dilution of a high vol.% MMC in a melt

Low **energy ball milling of Al and SiC powder**

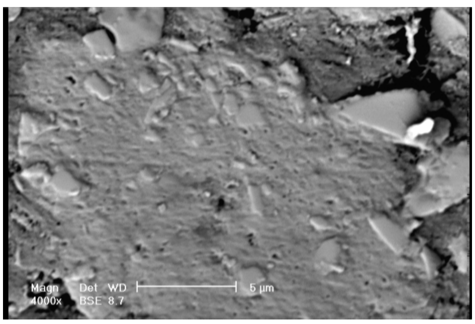

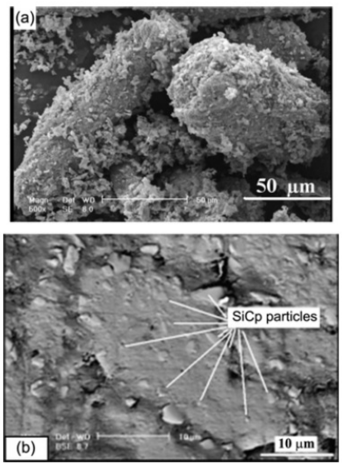

Fig. 3. SEM images of 24 hours milled composite powder: a) outer surface of the particles and b) cross section of the mounted powder.

M. Ghahremanian, et al., Met. Mater. Int., Vol. 18, (2012), pp. 149-156.

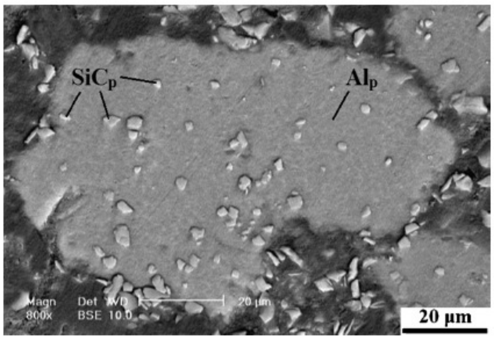

Fig. 3. SEM micrograph of cross section of $(Al–SiC_p)_{cp}$ composite particles.

S. Amirkhanlou, B. Niroumand / Materials Science and Engineering A, *(2011)*

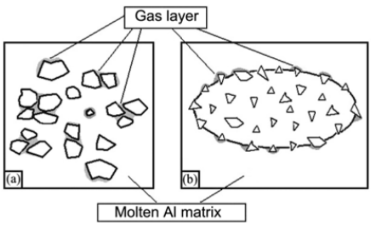

Fig. 4. Schematic of the expected gas layers around the SiC_p when the reinforcements are injected in the form of a) SiC_p powder and b) milled Al-SiC_p composite powder.

- Lower entrapped gas or gas layer
- Better Al-SiC_p contact (wettability)

Gradual reinforcement release mechanism

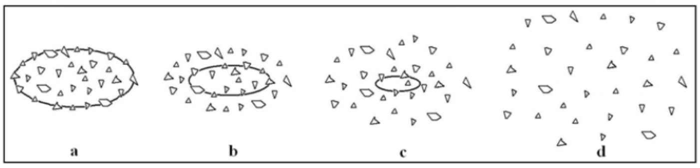

Fig. 5. Schematics of the expected gradual melting of a milled Al-SiC particle which results in gradual release and uniform dispersion of reinforcement particles in the melt.

M. Ghahremanian, et al., Met. Mater. Int., Vol. 18, (2012), pp. 149-156

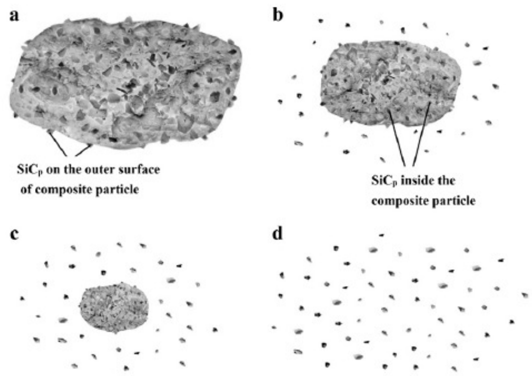

. Schematic of the expected gradual melting of a composite particle which results in gradual release and uniform dispersion of the reinforcement in the melt.

S. Amirkhanlou, B. Niroumand / Journal of Materials Processing Technology 212 (2012) 841– 847

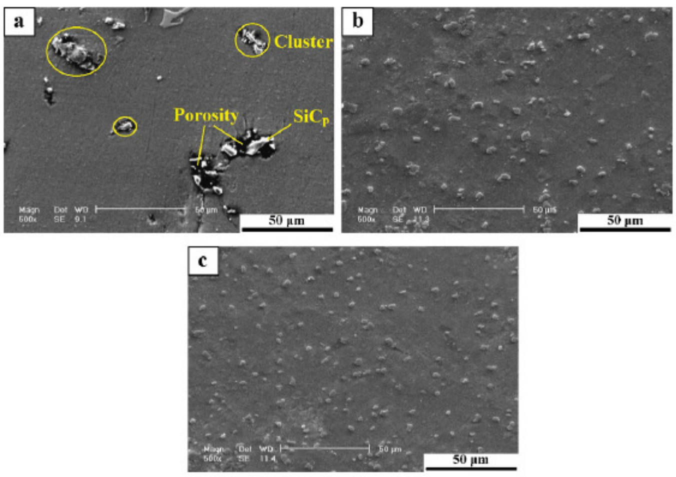

Fig. 6. Typical SEM microstructures of different samples: (a) Al356–SiC$_p$, (b) Al356–(Al–SiC$_p$)$_{cp}$, and (c) Al356–(Al–SiC$_p$–Mg)$_{cp}$.

S. Amirkhanlou, B. Niroumand / Journal of Materials Processing Technology 212 (2012) 841– 847

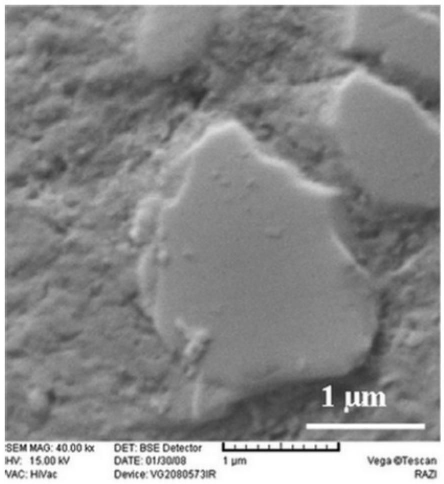

Fig. 7. SEM micrograph of the interface of a SiC_p with the matrix of sample 5.

M. Ghahremanian, et al, Met. Mater. Int., Vol. 18, (2012), pp. 149-156

Composite Materials, 2016, BN, IUT, Iran

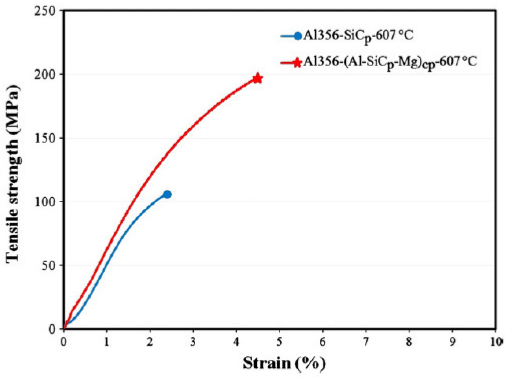

Fig. 5. Stress–strain curves for Al356–SiC_p–607 °C and Al356–(Al–SiC_p–Mg)$_{cp}$–607 °C composites.

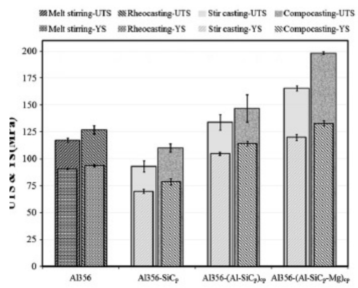

. 6. Comparison of UTS and 0.2% YS in monolithic and composite specimens.

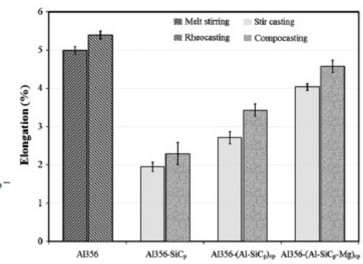

Fig. 7. Total elongation of monolithic and composite specimens.

S. Amirkhanlou, B. Niroumand , Materials and Design 32 (2011) 1895–1902

Composite Materials, 2016, BN, IUT, Iran

•Electroless co-deposition of P-Ni-CNT on Al or Mg particles to be injected into the melt

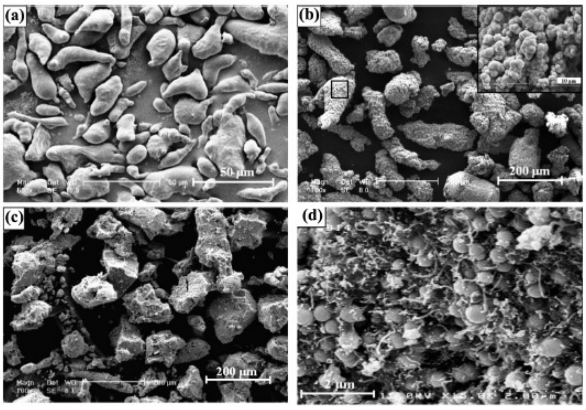

Fig. 3. SEM and FESEM micrographs of (a) as received Al powder, (b) Ni-P coated Al powder (bath No. 1) and (c-d) Ni-P-CNT coated Al powder with 1.25 g/lit CNT concentration in the bath (bath No. 3) at different magnifications.

B. Abbasipour, et al., Met. Mater. Int., Vol. 18, (2012), pp. 1015-21.

500 M. Firoozbakht et al. / Journal of Alloys and Compounds 509S (2011) S496–S502

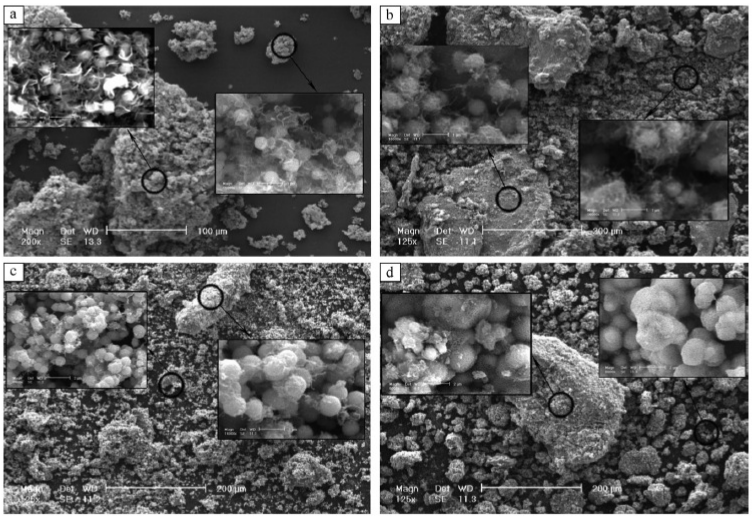

Fig. 7. SEM micrographs of composite coating on magnesium particles at magnesium powder/CNT weight ratios of (a) 1, (b) 2.5, (c) 4 and (d) 6.

CNT addition to the melt through ARBed Al-CNT composites

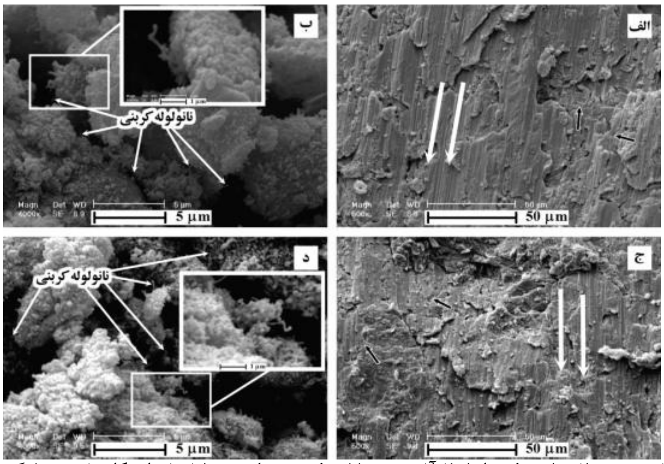

تصویر SEM از سطح برش حاصل از آزمون سوراخ برشی در دمای محیط نمونه‌های کامپوزیتی ریختگی:
الف) C0.5 - P0، ب) لبه های برجستگی های به وجود آمده در اثر برش نمونه C0.5 - P0،
ج) C0.5 – P160 و د) لبه های برجستگی های به وجود آمده در اثر برش نمونه C0.5 – P160.

Post casting deformation processes: Rolling, extrusion, …

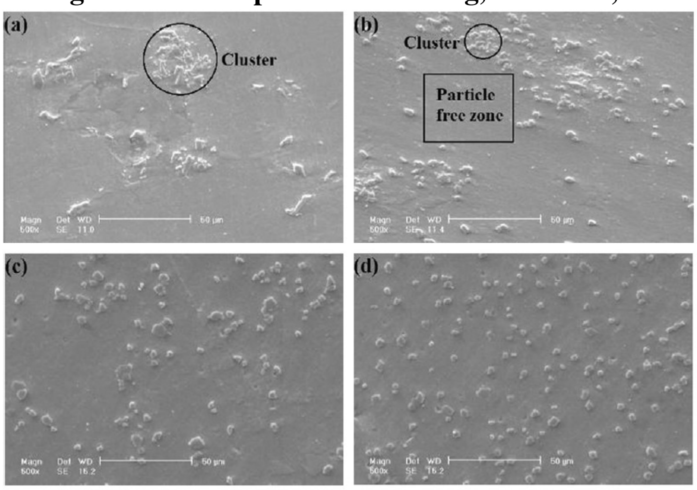

Fig. 2. SEM micrographs of the Al6061/10 vol.% SiC_p composite microstructures for: (a) 0% (as-cast), (b) 60%, (c) 85%, and (d) 95% reductions.

S. Amirkhanlou, et al., Materials and Design, 32 (2011) 2085–2090.

Particles redistribution during solidification

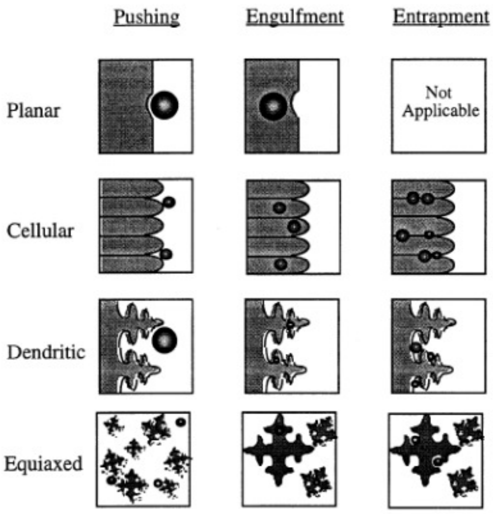

Particles redistribution during solidification

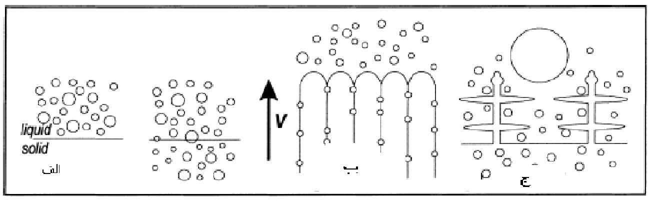

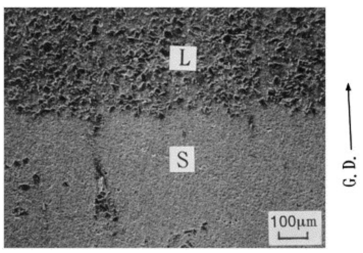

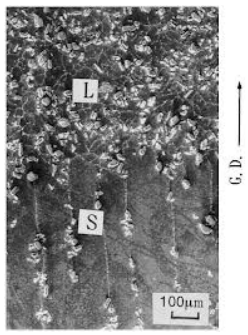

a-Particle pushing in Al-Al_2O_3
b- Particles entrapment in Al-Al_2O_3

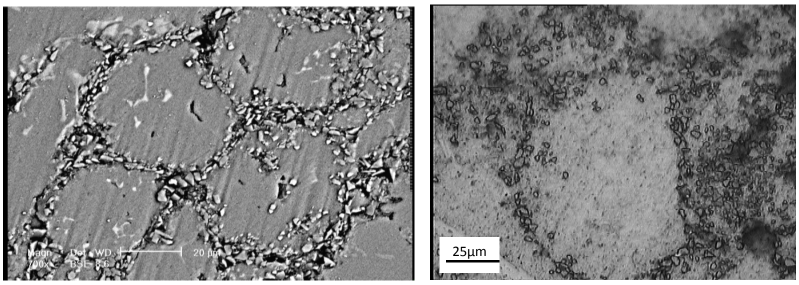

Particle entrapment in Al-SiC$_p$.

•Cooling rate (°C/sec) and solidification rate (mm/sec) affects the distribution

•Smaller DAS = more uniform distribution

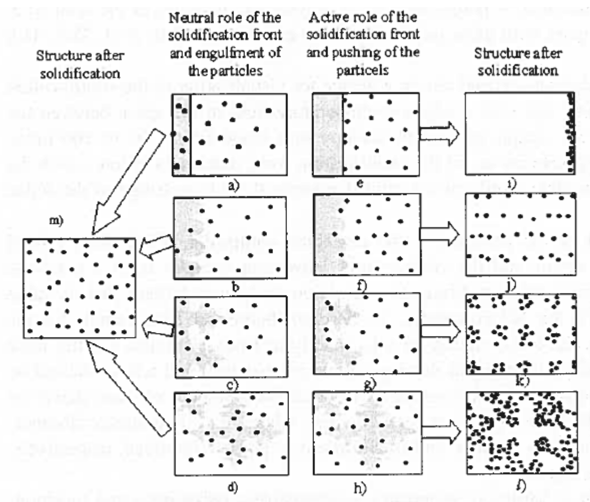

Fig. 1. Active/neutral role of the solidification front during its interaction with particles of an alien phase and the resulting structural effects; the solidification front during directional solidification: (a) planar, (b) cellular, (c) cellular-dendritic, (d) solidification in volume, (e), (i)÷(l) structure finally obtained

E. Fras, E. Olejnik, Archives of metallurgy and materials, Vol. 53, 2008,695-702.

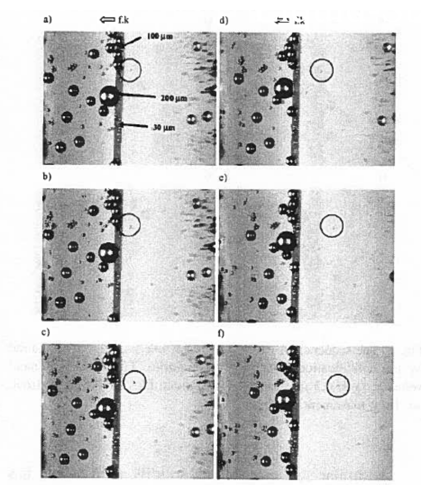

Fig. 4. The sequence in which the polystyrene particles are pushed by the solidification front in K1 composite. The front movement velocity (a,b) 0.05 µm/s; (c,d) 0.07 µm/s; (e,f) 0.08 µm/s. f.k – solidification front, ⇐ front movement direction

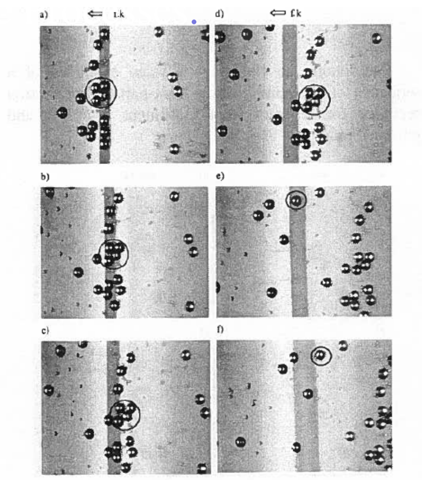

Fig. 5. The sequence in which the polystyrene particles are engulfed by the solidification front in K1 composite. The front movement velocity: (a-d) 0.5 µm/s and (e,f) 1.0 µm/s; f.k.- solidification front, ⇐ front movement direction

Succinonitrile/polystyrene composite slurry

E. Fras, E. Olejnik, Archives of metallurgy and materials, Vol. 53, 2008,695-702.

Forces acting onto a particle of radius R:

1. F= Buoyancy force

   •Negligible for small particles and can be disregarded!

2. F_σ= Surface tension force

3. F_η=Drag force

   •Caused by the viscosity (η) of the liquid

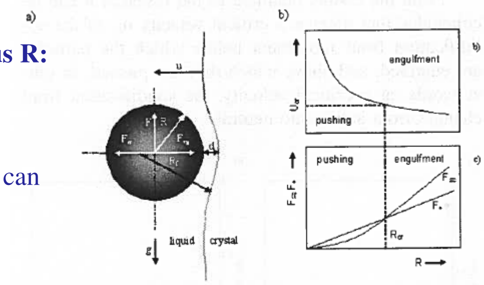

Fig. 11. Schematic representation of forces acting on a particle (a) and plotted curves of the critical velocity of the solidification front movement (b) and of the forces acting on a particle (c)

E. Fras, E. Olejnik, Archives of metallurgy and materials, Vol. 53, 2008,695-702.

$$F_\sigma = 2\pi R\Delta\sigma\left(\frac{a_0}{d}\right)^2\alpha$$

$$\alpha = \frac{R_f}{R_f - R}$$

a_0= the interatomic distance
d = the distance between the particle and the solidification front

R = Particle radius

R_f= Radius of solidification front curvature

$\Delta\sigma=\sigma_{PS} - \sigma_{PL}$
σ_{PS} = Particle-solid surface tension
σ_{PL} = Particle-liquid surface tension

•$\Delta\sigma>0 \rightarrow$ pushing is favored

•$\Delta\sigma<0 \rightarrow$ Engulfment is favored.
Less probable!
Particle acts as a nucleation site

$$F\eta = 6\pi\eta u\frac{R^2}{d}\alpha^2$$

u = Solidification front velocity
η = Absolute viscosity of the liquid

- If F_σ is pushing and is compensated by F_η at a constant u
  - $\rightarrow$ the particle is kept at a constant d from the solidification front
  - $\rightarrow$Velocity of the particle and that of the solidification front is the same
- If u is increased $\rightarrow$ F_η increases but F_σ remains the same!
  - $\rightarrow$ Ultimately resulting in a contact between the particle and the solidification front $\rightarrow$ Engulfment!

$F_\sigma - F_\eta = 0$ ⟶ $u_{cr} = \dfrac{a_o^2 \Delta\sigma}{3dR\alpha\eta}$

Assuming $d=a_0$ ⟶ $u_{cr} = \dfrac{a_o \Delta\sigma}{3R\alpha\eta} = \dfrac{A}{R}$

At a constant u:

$R<R_{cr}$ → Pushing

$R>R_{cr}$ → Engulfment

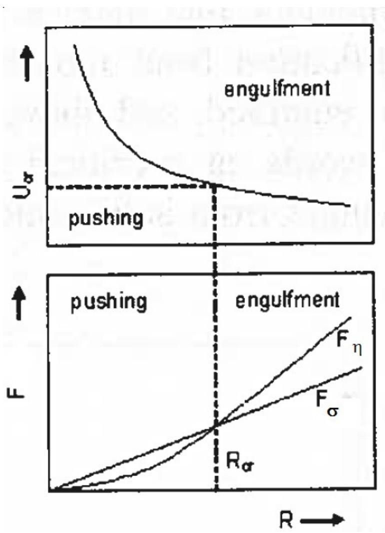

•Vc ∝Surface tensions, particle size, thermal properties of particles, …

For micron-sized particles:

Model	Critical Velocity for Engulfment	Dependence on Particle Radius
Uhlman et. al. [7]	$V = \frac{(n+1)}{2}\left(\frac{La_oV_oD}{k_BTR^2}\right)$	R^{-2}
Chernov et al. [8]	$V = \frac{0.14B_3}{\mu R}\left(\frac{\sigma_{sl}}{B_3R}\right)^{1/3}; \frac{\lambda^2}{l} > R$ $V = \frac{0.15B_3}{\mu Rl}; \frac{\lambda^2}{l} > R$	$R^{-1.33}$ $R^{-1.33}$
Bolling and Cisse [9]	$V = \left(\frac{4\psi(\alpha)k_BT\sigma_{sl}A_o}{9\pi\mu^2R^3}\right)^2; R < R_b$	$R^{-1.5}$
Stefanescu et al. [10]	$V = \frac{\Delta\sigma a_o}{6(n-1)\mu R}\left(2 - \frac{k_p}{k_l}\right)$	R^{-1}
Shangguan et al. [11]	$V = \frac{\Delta\sigma a_o}{6(n-1)\mu\alpha R}\left(\frac{n-1}{n}\right)^n$	R^{-1}
Kim and Rohatgi [6]	$V = \frac{\Delta\sigma a_o(kR+1)}{18\mu R}$	R^{-1}
Kaptay [12]	$V = \frac{0.157}{\eta}\Delta\sigma_{cls}^{2/3} \cdot \sigma_{sl}^{1/3} \cdot \left(\frac{a}{R}\right)^{4/3}$	$R^{-1.33}$

Table 1 Predictive Equations for Critical Velocity for Particle Engulfment during Solidification

3- Reinforcement/matrix wettability

I- Addition of certain elements such as Mg or Li to Al melts:

- Reduction in surface energy:
  - $\sigma_{Al} = 0.75\ NM^{-1}$
  - $\sigma_{Al\text{-}Si} = 0.817\ NM^{-1}$
  - $\sigma_{Mg} = 0.599\ NM^{-1}$
  - $\sigma_{Al} = 0.760\ NM^{-1}$ (at 740 °K)
  - $\sigma_{Al\text{-}3\%Mg} = 0.62\ NM^{-1}$ (at 740 °K)

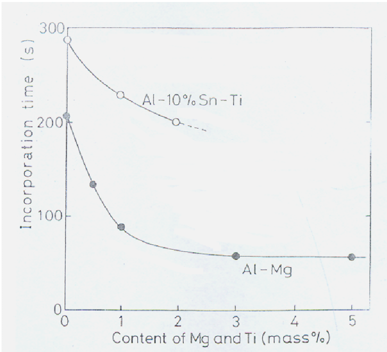

Effect of Mg% on incorporation time of SiC in Al.

- Formation of MgO, $MgAl_2O_4$, $LiAlO_2$, $Li_2Al_2O_4$ (on Al_2O_3) $\rightarrow$ Improved wettability

II- Reaction at the interface:

For example in Al/SiC systems:

$SiC \rightarrow (Si) + C$

$(Si)+mMe \rightarrow Me_mSi$

$(C)+nMe \rightarrow Me_nC$

$\rightarrow$ Improved wettability

III- Reinforcement coating

to improve wettability and adhesion and prevent reactions

- Boron fibers with SiC coating for use in Al alloys, CVD technique, 2-3 µm thick
- Boron fibers with B_4C coating for use in Ti alloys
- Carbon fibers with TiB_2, by CVD of Ti and Boron compounds, 20 nm
- Graphite particles with Ni or Cu coating
- …

IV- Effect of time and temperature on wettability

➢ Generally contact angle decrease with time and temperature

- Contact angle of Al and Al_2O_3:
  - 180° at melting point of Al (no wetting)
  - 60 ° at 1800 °K

Effect of time and temperature on wettability of SiC in aluminum melt.

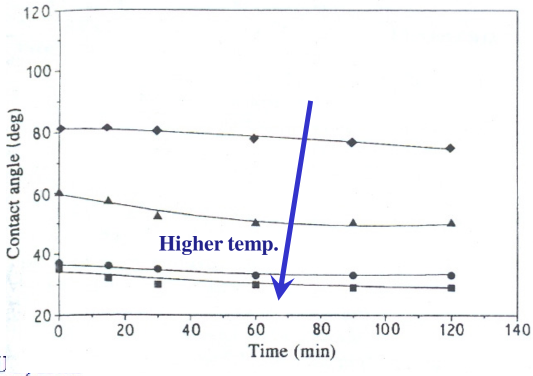

4-Undesirable reactions between reinforcement/matrix

- Such as formation of Al_4C_3 in Al/SiC composites

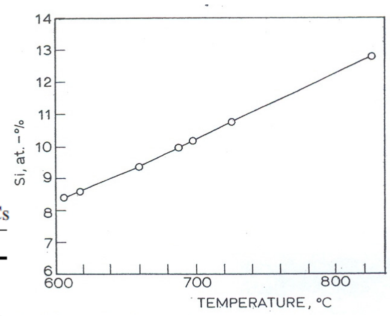

Minimum Si% required to avoid Al_4C_3 formation at different temperatures

Table 6.3 Interfacial reaction products in some important MMCs

Reinforcement	Matrix	Reaction product(s)
SiC	Ti alloy	TiC, Ti_5Si_3
	Al alloy	Al_4C_3
Al_2O_3	Mg alloy	MgO, $MgAl_2O_4$ (spinel)
C	Al alloy	Al_4C_3
B	Al alloy	AlB_2
Al_2O_3 + ZrO_2	Al alloy	$ZrAl_3$
W	Cu	None
C	Cu	None
Al_2O_3	Al	None

Composite Materials, 2016, BN, IUT, Iran

Interface Reactions of Aluminum with Carbon Fibers

Carbon fiber / Al Si6 - interface (TEM analysis):

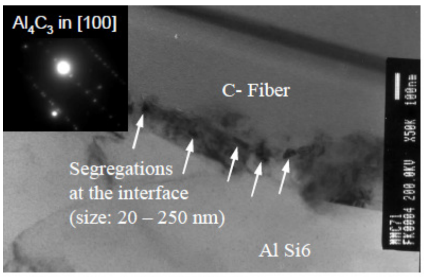

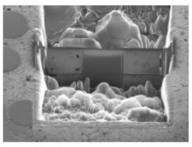

TEM lamella (d = 100–200 nm) (prepared by focussed ion beam)

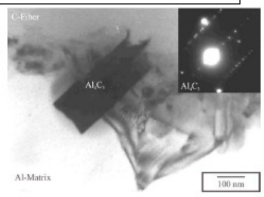

acc: K. von Niessen et al., Paper # 23-3, Proceedings 8th Int. Conference on Semi-Solid Processing of Alloys and Composites, S2P 2004 (Limassol, Cyprus, September 21–23, 2004). Published by NADCA, Wheeling, Illinois, USA

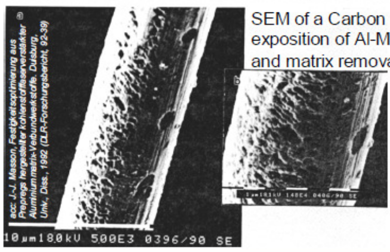

SEM of a Carbon fiber after thermal exposition of Al-MMC (650°C, 10 min) and matrix removal with sodium hydroxide

Possible reaction products and precipitates:
- Al_4C_3
- Mg_2Si
- Al_2MgO_4
- others, depending on alloying elements
- free Si

IFKB University of Stuttgart   S2P   Innovations in Metal Matrix Composite Processing   R. Gadow IFKB P-727 slide 17

Interface Reactions with Ceramic Reinforcements

Chemical interface reaction products in Al Mg4 / SiC$_p$ (Squeeze Casting):

a) Al_4C_3
b) Mg_2Si

→ Cu-alloying (AlCuMgAg matrix, T6) yields best mechanical results (σ_f = 700 MPa, K_{Ic} = 9.5 MPa·m^{½}) due to load dislocation by ductile matrix.

acc: O. Beffort et al., In: Verbundwerkstoffe (14. Symposium Verbundwerkstoffe und Werkstoffverbunde, Wien, 2003), H. P. Degischer (ed.). Weinheim : Wiley-VCH, 2003, p. 61–66

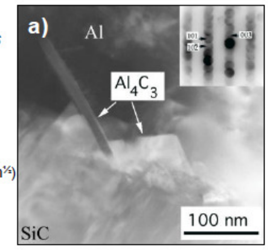

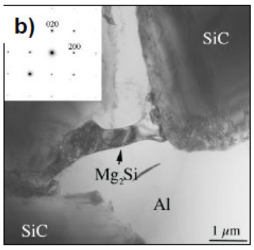

Reaction products after thermal exposition for ceramic oxide (Al_2O_3) fibers:

acc: S.Vaucher, O.Beffort, MMC-Assess Thematic Network Report, Volume 9, Thun/Wien, 2001

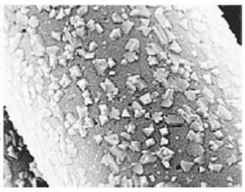

loss of → mech. properties

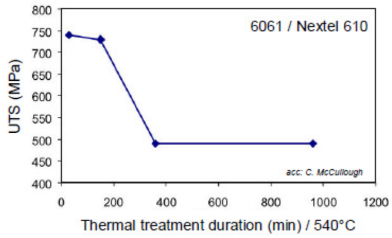

$MgAl_2O_4$ crystals on Nextel 610 fiber surface
(extracted from EN AW-6061, heat treated at 540°C / 16 h; courtesy of 3M)

IFKB University of Stuttgart | S2P | Innovations in Metal Matrix Composite Processing | R. Gadow IFKB P-727 | slide 18

Properties

- **Young's Modulus**

✓ Unidirectionally reinforced continuous fiber reinforced MMCs:
   – A linear increase in the longitudinal Young's modulus as a function of the fiber volume fraction (in agreement with the rule-of-mixtures)
   – The modulus increase in a direction transverse to the fibers is very low.

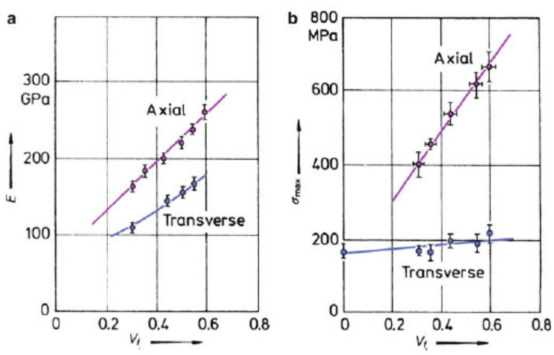

Fig. 6.19 Properties of Al_2O_3/Al–Li composites as a function of fiber volume fraction (V_f): (a) axial and transverse Young's modulus vs. fiber volume fraction, (b) axial and transverse ultimate tensile strength vs. fiber volume fraction. [From Champion et al. (1978), used with permission]

Composite Materials,

Properties

- Particle reinforced MMCs :
  - Increased modulus
  - The increase is much less than that predicted by the rule-of-mixtures
  - The stiffness enhancement in particulate composites is reasonably isotropic

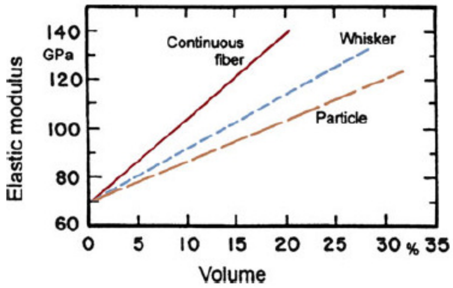

Fig. 6.20 Increase in Young's modulus of an MMC as a function of reinforcement volume fraction for continuous fiber, whisker, or particle reinforcement

Properties

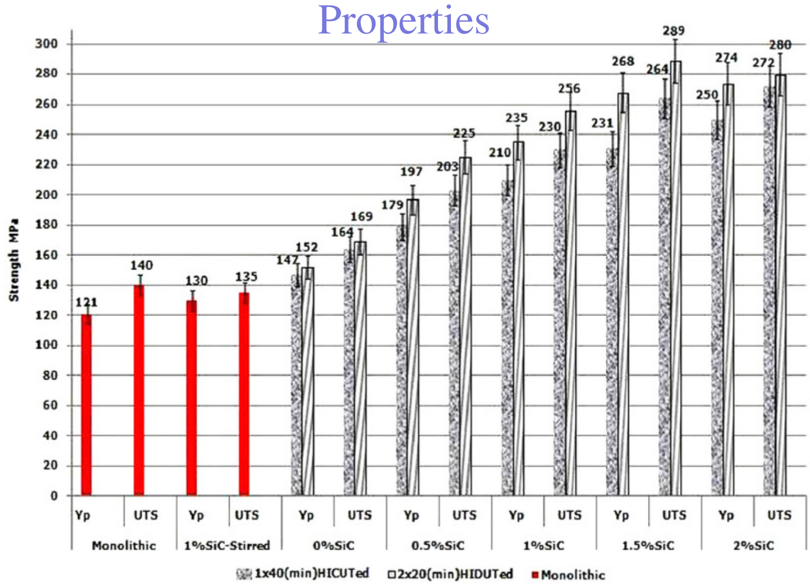

Fig. 12. Comparison between yield and ultimate tensile strengths of HICUTed and HIDUTed samples after 40 min of total treatment time.

 Dehnavi, et al., Materials Science & Engineering A, 617(2014)73-83.

Properties

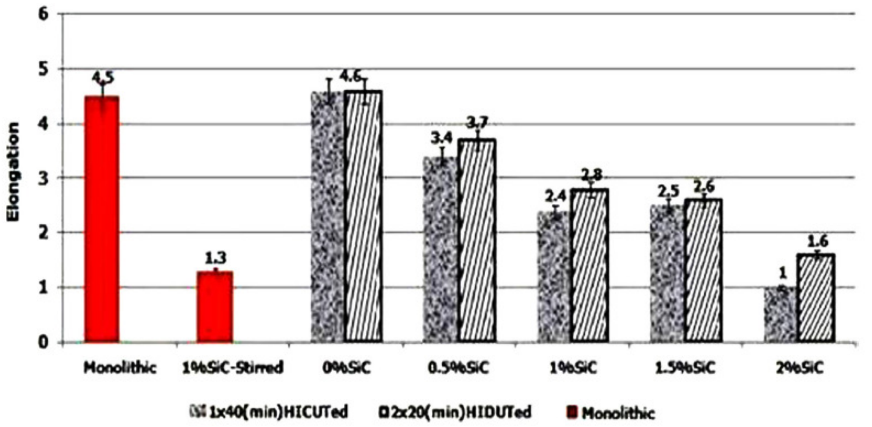

Fig. 13. Comparison between elongation values of HICUTed and HIDUTed samples after 40 min of total treatment time.

M.R. Dehnavi, et al., Materials Science & Engineering A, 617(2014)73–83.

Properties

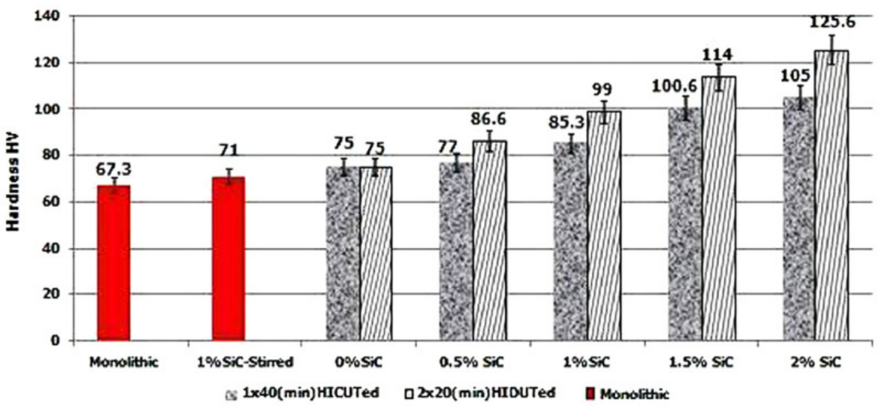

Fig. 14. Comparison between hardness values of HICUTed and HIDUTed samples after 40 min of total treatment time.

M.R. Dehnavi, et al., Materials Science & Engineering A, 617(2014)73–83.

Properties

➢ Strengthening mechanisms in metal matrix composites

➢ **Direct strengthening:**

– Considers only the contribution of the reinforcement and the matrix (load transfer from the matrix to high modulus reinforcements)

– Is critically dependant on the reinforcement-matrix interface

– Does not take into account any strength contribution from microstructural changes in the metal matrix

- For fiber reinforced MMCs:
  - Rule of mixtures: $\sigma_c = \sigma_f V_f + \sigma_m V_m$
    - σ = the strength
    - V = the volume fraction
    - c, f, and m denote the composite, fiber, and matrix, respectively

➢Strengthening mechanisms in metal matrix composites

• For particle reinforced MMCs:

$$\Delta\sigma_l = v_p \sigma_m \left[\frac{(l+t)A}{4l}\right]$$

$\Delta\sigma_l$ = load-bearing contribution of reinforcement
v_p = volume fraction of particles in the matrix
σ_m = yield strength of the matrix
l = size of the particulate parallel to the load direction
t = thickness of the particulate, and
A = l/t = particles aspect ratio

•For equiaxed (spherical) particles:

$$\Delta\sigma_l = 0.5 v_p \sigma_m$$

A. Sanaty-Zadeh, P.K. Rohatgi, Materials Science and Engineering A 531 (2012) 112– 118.

➢Strengthening mechanisms in metal matrix composites

- **Indirect strengthening:**
  - The reinforcement-induced changes in matrix microstructure and properties including:
    - Orowan strengthening
    - Grain and substructure strengthening
    - Quench hardening
    - Work hardening
    - Solid solution strengthening

- The indirect strengthening appears to be more important in particle reinforced composites.

➢Strengthening mechanisms in metal matrix composites

- **Orowan strengthening**

- Hard and non-shearable particles may pin and block the dislocations.
- Orowan effect= Gb/l
  - G = shear modulus of the matrix
  - b = Burgers vector of the matrix
  - l = particle spacing

- The degree of strengthening is believed to be insignificant for micro-sized reinforcements.
- Nano MMCs seem to benefit more from this mechanism.

- Presence of reinforcements often affects the size and distribution of second phase precipitates.

➢Strengthening mechanisms in metal matrix composites

➢ **Grain and substructure strengthening**

- Hall–Petch relationship:

$$\sigma_y = \sigma_0 + \frac{k_y}{\sqrt{d}}$$

- σ_y = yield strength
- σ_0 = a materials constant (resistance of the lattice to dislocation motion)
- k_y = the strengthening constant
- d = grain or sub-grain size in the matrix.

- Grain boundary strengthening can be high in spray cast and powder metallurgy processed composites.

➢Strengthening mechanisms in metal matrix composites

A356-2%CNT

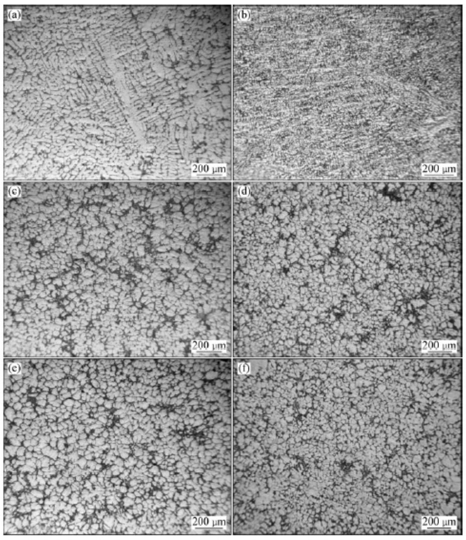

Fig.5 Typical micrographs of cast samples: (a) A-0-0; (b) A-0-2; (c) A-15-0; (d) A-15-2; (e) A-30-0; (f) A-30-2

Abasipour, B., et al., Transactions of Nonferrous Metals Society of China, 20, (2010) 1561-1566.

➢Strengthening mechanisms in metal matrix composites

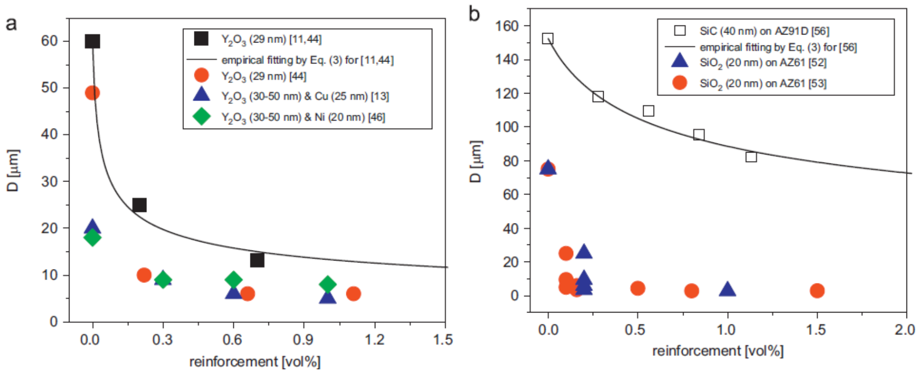

Fig. 3. Influence of reinforcement particle vol% on the matrix grain size refinement of Mg MMNCs, (a) influence of Y_2O_3 on pure Mg MMNCs, and (b) influences of SiO_2 and SiC on alloy Mg MMNCs.

J.B. Ferguson, et al., Materials Science & Engineering A, 558 (2012) 193–204.

➢Strengthening mechanisms in metal matrix composites

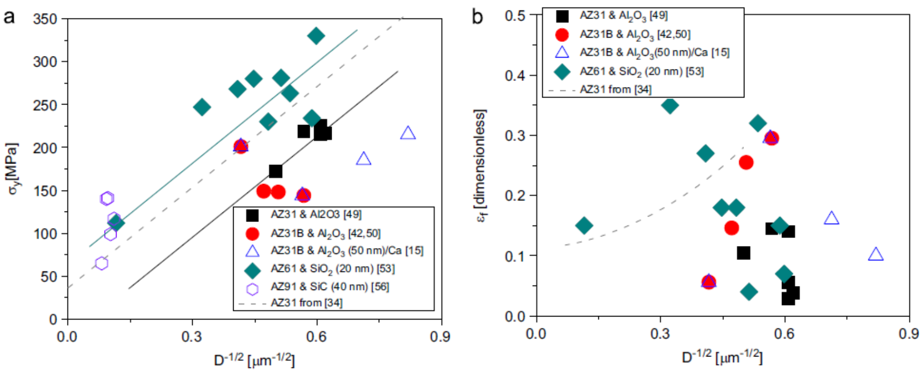

Fig. 7. Influence of Al_2O_3, SiO_2, and SiC concentrations and inverse square root of grain size on the (a) yield strength (σ_y) and (b) strain to failure (ε_f) of Mg alloy MMNCs. (For interpretation of the references to color in this figure legend, the reader is referred to the web version of this article.)

J.B. Ferguson, et al., Materials Science & Engineering A, 558 (2012) 193–204.

➢Strengthening mechanisms in metal matrix composites

- **Quench hardening** .

- Reinforcements normally have smaller coefficient of thermal expansions (CTEs) than the matrix
- When subjected to a temperature change, thermal stresses are generated in both of the components
- A metal matrix undergoes plastic deformation in response to the thermal stresses generated and thus alleviates them
- A high density of dislocations may be generated around the reinforcements

➢Strengthening mechanisms in metal matrix composites

Alumina fiber/Mg alloy matrix

Twins in Mg matrix →
plastic deformation in Mg
due to thermal stresses

RZ= reaction zone

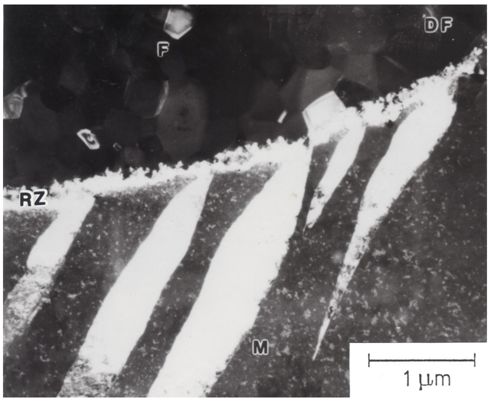

➢Strengthening mechanisms in metal matrix composites

•A dislocation etch-pitting technique was used to delineate dislocations in single crystal copper matrix (1975).

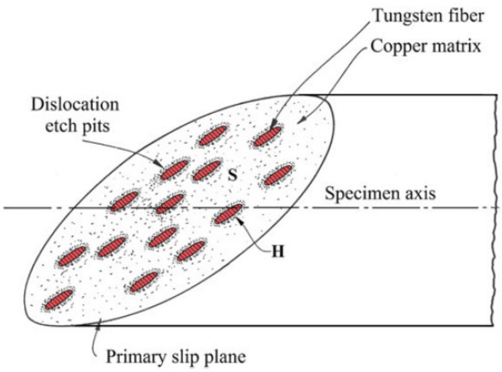

Fig. 6.16 A primary plane section of a metal matrix composite is shown as having a hard zone (high dislocation density) around each fiber and a soft zone (low dislocation density) away from the fiber

➢Strengthening mechanisms in metal matrix composites

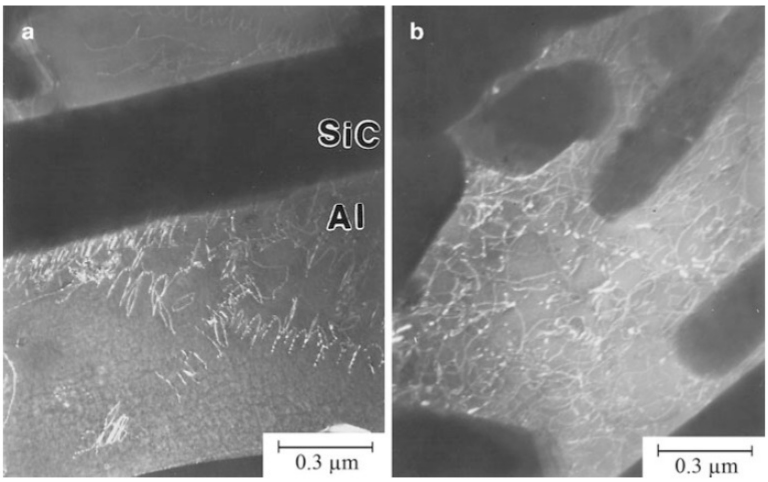

Fig. 6.26 Dislocation distribution in the aluminum matrix of a SiC_w/Al composite: (**a**) inhomogeneous dislocation distribution before testing, (**b**) uniform dislocation distribution after fatigue testing. [From Williams and Fine (1985a), used with permission]

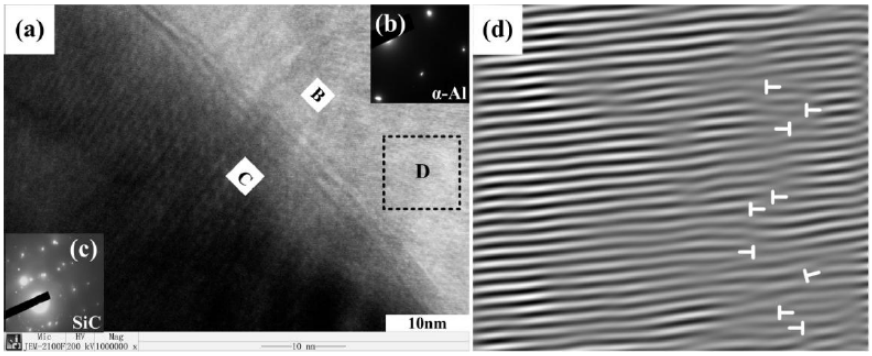

Fig. 6. (a) The HRTEM image of the interface between the nano-SiC particle and the matrix in the 0.5 vol.% nano-SiC$_p$/Al2014 composites, (b) the selected area electron diffraction (SAED) pattern at the area B, (c) SAED pattern at the area C, (d) IFFT image of the zone D.

IFFT: Inverse Fast Fourier transform

Long-Jiang Zhang, et al., Submitted to Materials Characterization, 2014

➢Strengthening mechanisms in metal matrix composites

- Thermal strain in the matrix: $e_m = \Delta\alpha\Delta T$

– The dislocation density resulting from CTE mismatch:

$$\rho_{CTE} = (AeV_p)/b(1 - V_p)d$$

- – A = a geometric constant
- – e = the thermal misfit strain
- – b = the Burgers vector
- – V_p = the particle volume fraction
- – d = the particle diameter

- The strength contribution is given by

$$\sigma_q = \alpha Gb(\rho_{CTE})^{1/2}$$

α = a constant
G = the shear modulus of the matrix

➢Strengthening mechanisms in metal matrix composites

- Accelerated aging processes due to heterogeneous nucleation at dislocations

- This contribution of quench hardening to strength can be significant.

➢Strengthening mechanisms in metal matrix composites

➢ **Work hardening**

- Due to the modulus mismatch (strain misfit) between the elastic reinforcement and the plastic matrix

- Reinforcements affect the matrix work hardening rate.

✓ Effect of modulus mismatch on the strength of a composite:

$$\sigma_d = \sqrt{3}\alpha G b \sqrt{\rho^{EM}}$$

- α = a constant (~0.5)
- ρ^{EM} = the dislocation density caused by modulus mismatch
- G = the shear modulus of the matrix
- b = the Burger's vector

$$\rho^{EM} = \frac{6 v_p}{\pi d_p^3} \varepsilon$$

- v_p= volume fraction of particles
- d_p = the particle diameter
- ε= the uniform deformation

A. Sanaty-Zadeh, P.K. Rohatgi, Materials Science and Engineering A 531 (2012) 112– 118.

➢Strengthening mechanisms in metal matrix composites

- **Solid solution strengthening**

- The reinforcements may affect the microsegregation as a result of solute segregation at the interfaces or chemical reaction with the matrix.

→ The content and distribution of solute in the matrix is changed

➢Strengthening mechanisms in metal matrix composites

- In MMCs reinforced with continuous fibers, direct strengthening is a major factor.
- For discontinuously reinforced metals, quench hardening and work hardening are likely to be the most active mechanisms.
- For nano-sized reinforcements, Orowan strengthening may become a key mechanism.
- Normal matrix strengthening due to solution and precipitation hardening and grain refinement will give additional strength to the composite.

+ The strength of MMCs is most strongly dependent on the volume fraction of reinforcement.

➢Strengthening mechanisms in metal matrix composites

The overall strength of the composite:

•There are different models. Two examples:

1- Simply add up all the strengthening contributions:
- •Neglects the effect of different mechanisms on each other
- •Assumes that each mechanism behaves independently

$$\sigma = \sigma_0 + \Delta\sigma_1 + \Delta\sigma_2 + \Delta\sigma_3 + \Delta\sigma_4 + \cdots$$

2- Clyne method (for micro composites):

$$\sigma_y = \sigma_0 + \Delta\sigma$$

$$\Delta\sigma = \sqrt{(\Delta\sigma_l)^2 + (\Delta\sigma_{Orawan})^2 + (\Delta\sigma_{Hall-Petch})^2 + (\Delta\sigma_{EM})^2 + (\Delta\sigma_{CTE})^2 + (\Delta\sigma_{WH})^2}$$

σ_0 = Yield strength of the unreinforced matrix

A. Sanaty-Zadeh, P.K. Rohatgi, Materials Science and Engineering A 531 (2012) 112– 118.

➢Strengthening mechanisms in metal matrix composites

Mg MMCs reinforced with nano Al_2O_3 particles

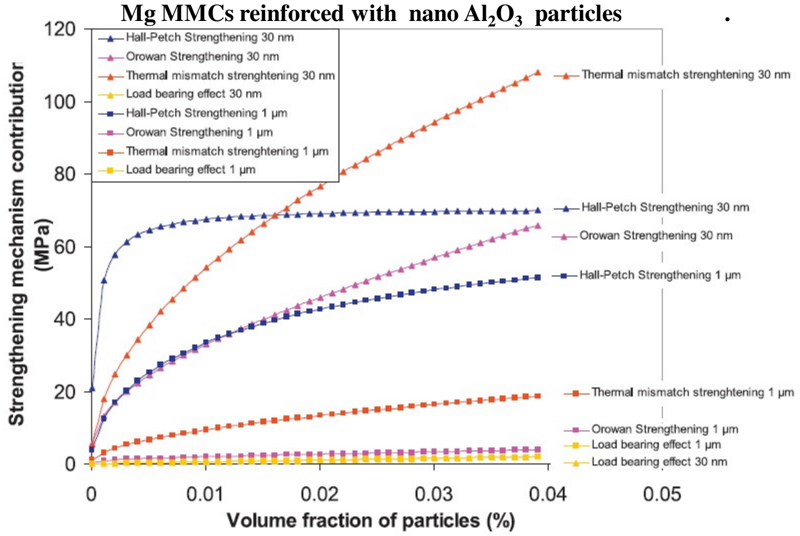

Fig. 7. Strengthening mechanism contributions as a function of volume fraction for the particle sizes 10 nm and 1 μm.

Sanaty-Zadeh, Rohatgi, Materials Science and Engineering A 531 (2012) 112- 118.

➢Strengthening mechanisms in metal matrix composites

- For Mg matrix reinforced with nano-Al_2O_3 and Y_2O_3 particles
  - ✓ There is a 75 nm particle size threshold
  - ✓ Larger particle sizes do not significantly influence the strength of the nanocomposite.

- Theoretical calculation in Prof. Rohatgi's group:
  - ✓ An ideal Al-15vol% Al_2O_3 (10 nm particles)
    - ✓ → **1GPa yield strength!**

Properties

High-temperature mechanical properties:

- Retention of mechanical properties at high-temperature is one of the main characteristics of high performance MMCs.

SiCw (21% V_f)/2024 Al composites

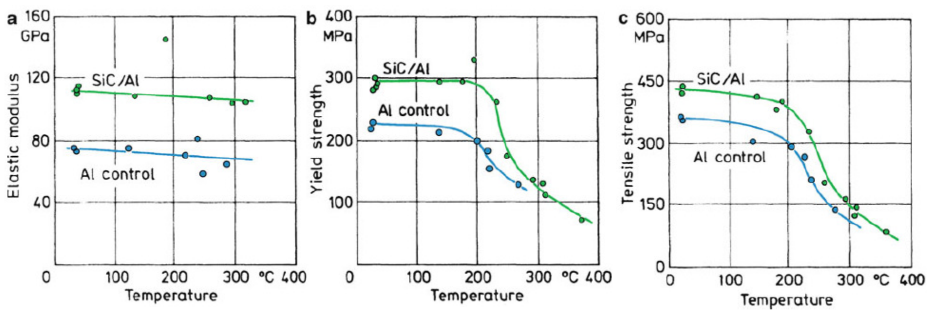

Fig. 6.24 Comparison of high-temperature properties of SiC_w/Al composites and aluminum: (**a**) elastic modulus, (**b**) yield stress, (**c**) ultimate tensile strength. [From Phillips (1978), used with permission]

Properties

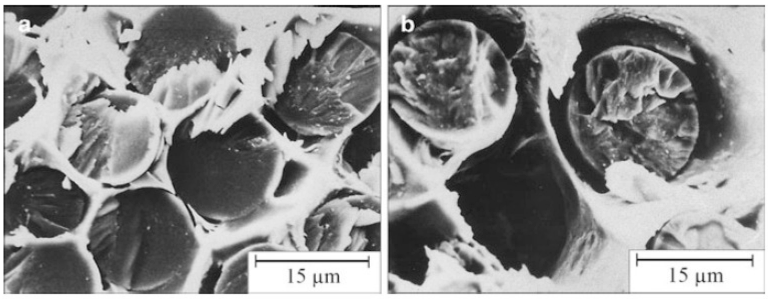

Fig. 6.25 Tensile fracture in Nicalon fiber/aluminum: (**a**) at room temperature showing a planar fracture, (**b**) at 500 °C showing fiber/matrix separation and fiber pullout leaving a hole. [Courtesy of K. Okamura]

Loss of adhesion between the fibers and the matrix at 500°C

→ Fiber/matrix separation and fiber pullout

Properties

Cast Al356/5vol.% SiCp (3 μm diameter)

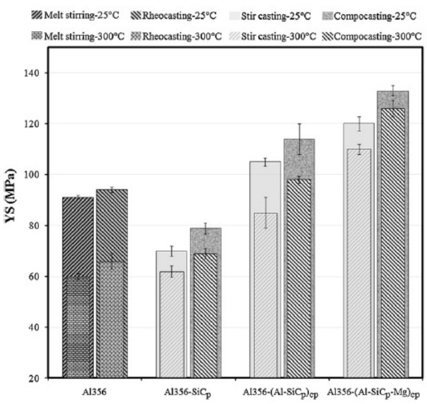

Fig. 7. Comparison of YS of monolithic and composite specimens at 25 °C and 300 °C.

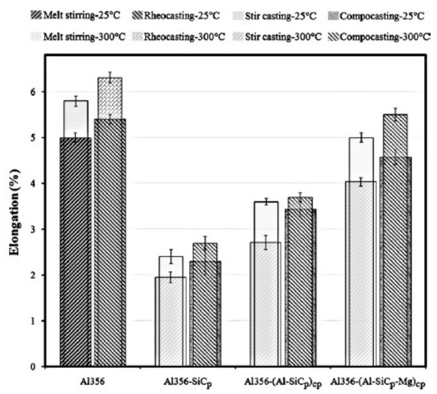

Fig. 8. Comparison of total elongation of monolithic and composite specimens at 25 °C and 300 °C.

S. Amirkhanlou, B. Niroumand, Materials Science and Engineering A 528 (2011) 7186– 7195.

Properties

A356-2vol% CNT

Table III. 0.2% Ys of the cast samples at 25 and 300 °C as well as the percentage of the retained yield strength at 300 °C.

Sample	Ys at 25 °C (MPa)	Ys at 300 °C (MPa)	Retained yield strength at 300 °C (%)
A-0-0	92	56	60
A-0-2	128	146	82
A-15-0	98	70	71
A-15-2	143	125	87
A-30-0	113	79	71
A-30-2	158	142	90

A-X-Y

X= 0 → Cast from fully liquid state
X= 15 → Cast from semi solid state ($f_s = 0.15$)
X= 30 → Cast from semi solid state ($f_s = 0.30$)

Y=0 → 0% CNT (Monolithic)
Y= 2 → 2% CNT (Composite)

B. Abbasipour, et al., Proceedings of TMS conference, Vol. 1, 2012, 733-740.

Recycling of MMCs

- **Recycling of MMCs as MMCs**, i.e., without separating the reinforcement from the matrix
  - Very economical if possible!
  - Must avoid excessive thermal treatments because they can cause adverse chemical interactions at the interface.
  - High Si content Al alloys can be recycled and reused (less chance of carbide formation)
  - Addition of virgin metal to the composite scrap may be required to obtain a new composite with the desired particle volume fraction.

- **Separation of the original components**
  - Mechanical or chemical techniques

Recycling of MMCs

- **Mechanical techniques**
  - Separating the metal and ceramic particles by mechanical means such as crushing, shredding, and gravity separation can be used.
- **Chemical techniques**
  - Special fluxing and degassing techniques
  - Fluxes, based on NaCl, KCl, and NaF are used in foundries for removing impurities from molten nonferrous metals such as aluminum.
  - Fluxing materials should have lower surface energies with the ceramic reinforcement than with the metal matrix
  - Al can be reclaimed from scrap by melting at 700^{o}C and adding fluxing salt and bubbling argon through the melt to form froth that concentrates alumina or SiC particles dewetted by the salt

Recycling of MMCs

Fig. 6.30 Chemical action of fluxing materials to separate the metal matrix from fiber or particle [after Nishida 2001]